GEOPHYSICAL RESEARCH LETTERS, VOL. 39, L14806, doi:10.1029/2012GL052245, 2012

On the spatial distribution of high winds off southeast Greenland

B. E. Harden[1] and I. A. Renfrew[1]

Received 9 May 2012; revised 18 June 2012; accepted 19 June 2012; published 31 July 2012.

[1] The spatial distribution of barrier winds along southeast Greenland has been investigated through idealized modeling of unidirectional flow towards an isolated mountain. The regions of enhanced surface wind speed seen in previous studies are reproduced and shown to be primarily the result of promontories in the orography along the southeast coast (the maxima disappear in experiments without the promontories). Two mechanisms are proposed to explain these enhancements. Firstly, a reduction in pressure experienced by the flow as it passes a promontory results in an acceleration akin to that of easterly tip jets at Cape Farewell. Secondly, mountain waves observed along the southeast coast are accompanied by strong, low-level downslope winds in the lee of the promontories. Both mechanisms contribute to the simulated wind speed maxima. **Citation:** Harden, B. E., and I. A. Renfrew (2012), On the spatial distribution of high winds off southeast Greenland, *Geophys. Res. Lett.*, *39*, L14806, doi:10.1029/2012GL052245.

1. Introduction

[2] The coastal regions of Greenland are renowned for experiencing a multitude of low-level, intense wind phenomena [*Moore and Renfrew*, 2005; *Renfrew et al.*, 2008] such as tip jets at Cape Farewell [*Renfrew et al.*, 2009; *Våge et al.*, 2009] and barrier winds along the southeast coast [*Petersen et al.*, 2009; *Harden et al.*, 2011]. These phenomena are formed through the distortion and deflection of the synoptic flow by Greenland's high and broad topography. They are so strong and frequent that they make the seas to the south of Greenland the stormiest in the world's oceans [*Moore et al.*, 2008].

[3] Here we focus on the barrier winds that form along the southeast coast of Greenland when stable air is forced towards the high, steep slopes. Unable to ascend the topography, the air is dammed and forced to flow to the left, down the coast in a strong, near-surface jet. These have been studied in the past decade through in situ data [*Petersen and Renfrew*, 2009; *Petersen et al.*, 2009], high resolution modeling [*Petersen et al.*, 2009], satellite derived winds [*Moore and Renfrew*, 2005] and reanalysis [*Harden et al.*, 2011]. These studies have shown that winds stronger than 20 m s^{-1} are a weekly wintertime occurrence and that the jets can exhibit complex dynamics. Barrier winds are also capable of producing large heat and momentum fluxes which can influence the ocean in a number of ways. For example, barrier winds can drive warm waters up Greenland fjords, undercutting glacial tongues and aiding the descent of the ice flow into the ocean [*Straneo et al.*, 2010]; can increase oceanic mixed layer depths [*Haine et al.*, 2009]; and have been shown to be a driver for the cross shelf transfer of dense water into the East Greenland Spill Jet [*Harden*, 2012].

[4] A consistent feature seen in both QuikSCAT and reanalyses is the uneven distribution of the barrier winds along the southeast coast [*Moore and Renfrew*, 2005; *Harden et al.*, 2011]. Specifically, there are two regions which are more frequently hit by strong barrier winds (Figure 1) and which experience wind speed peaks [*Harden et al.*, 2011]. The reason for this distribution is currently not understood. Addressing this problem will augment understanding of barrier wind dynamics, improve predictability, and aid interpretation of their impact on the ocean.

[5] The aim of this study is therefore to investigate the reasons for the spatial distribution of Greenland barrier winds and propose possible forcing mechanisms. *Moore and Renfrew* [2005] speculated that outflow from fjords may have a role to play and that the presence of Iceland allows a 'gap flow' mechanism, although the latter's influence was deemed small by *Petersen et al.* [2009]. Another potential factor could relate to the cyclones responsible for the barrier winds such as locational preference and 3-D structure; the development of barrier winds has been shown to be influenced by both the particular synoptic situation [*Petersen et al.*, 2009] and the state of the North Atlantic storm track [*Harden et al.*, 2011]. Here, though, we examine the hypothesis that the spatial distribution of barrier winds is primarily dictated by the local orography. Figure 1 shows that the two regions of enhanced barrier wind activity occur just offshore of the two major promontories along the southeast coast of Greenland. A geometrical argument therefore suggests that the precise shape of the southeast coast of Greenland may be a factor in determining the regions of the strongest barrier wind activity. This will be tested through idealized numerical simulations of unidirectional flow towards an isolated mountain representative of Greenland.

2. Experimental Setup

[6] The Met Office Unified Model version 7.5 was run in idealized mode for this study. This version employs a non-hydrostatic, fully compressible, deep atmosphere with a semi-Lagrangian treatment for advection of all prognostic variables except density which is given a Eulerian treatment. The model is discretized with Arakawa C grid staggering in the horizontal and Charney-Philips grid staggering in the vertical. Time stepping is through a predictor-corrector, two-time-level, semi-implicit scheme. This model has been shown in previous studies to adequately represent the range

[1]School of Environmental Sciences, University of East Anglia, Norwich, UK.

Corresponding author: B. E. Harden, School of Environmental Sciences, University of East Anglia, Norwich NR4 7TJ, UK. (b.harden@uea.ac.uk)

0094-8276/12/2012GL052245

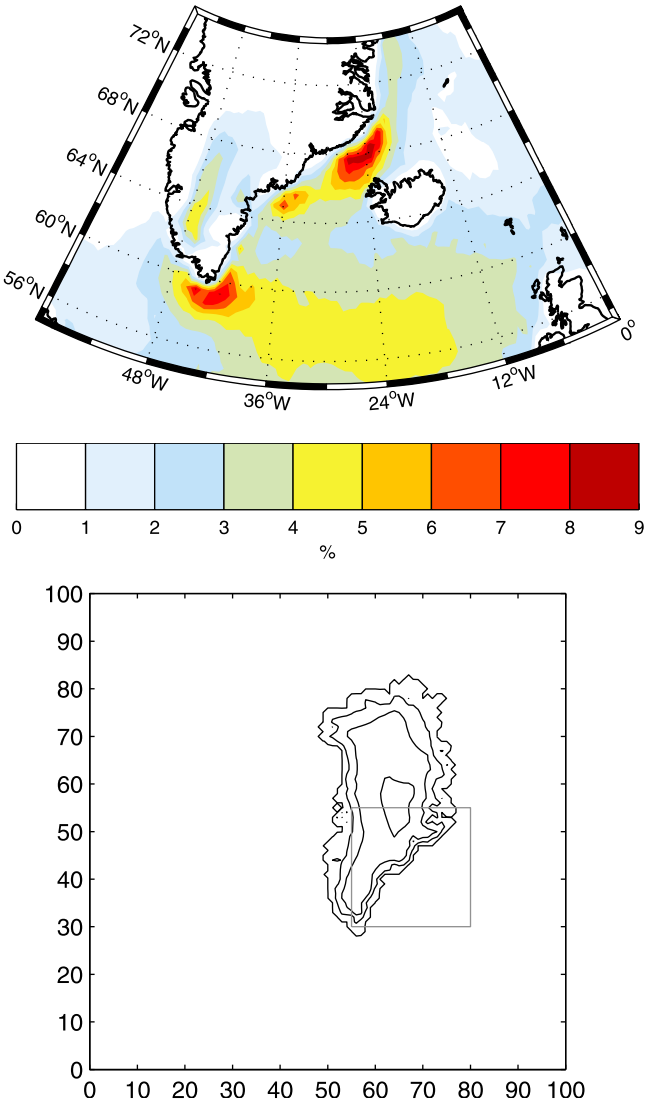

Figure 1. (top) Percentage of time the 10-m wind speed is greater than 20 m s^{-1} from ECMWF reanalysis ERA-Interim as *Harden et al.* [2011]. (bottom) Model domain for the idealized experiments with realistic orography contoured every 1000 m. The inner box indicates the domain presented in subsequent figures.

of low-level strong wind jets found around Greenland [*Petersen et al.*, 2009; *Outten et al.*, 2009].

[7] The model was set up in Cartesian coordinates on an f-plane (latitude 68°N, f = 1.35 × 10^{-4} s^{-1}) with a horizontal resolution of 48 km spaced over 100 × 100 grid points. The two wind speed maxima under investigation were apparent in the 80 km resolution ERA-Interim reanalysis [*Harden et al.*, 2011] implying that a resolution of 48 km should be adequate to resolve the processes responsible for the wind speed enhancements. There were 72 non-uniformly spaced, terrain-following sigma levels in the vertical. A time step of 60 seconds was used for all the experiments and the model was run with no moist processes. The lower boundary conditions were no flux and free slip, and a gravity wave damping scheme was employed at the upper boundary.

[8] The model domain is shown in Figure 1 (bottom) along with the isolated mountain representing the 48 km resolution orography of Greenland derived from GLOBE [*Hastings et al.*, 1999] used in the experiments. The model was initialized everywhere with a constant velocity, in geostrophic balance with the pressure and temperature fields. There was an initial constant static stability throughout the domain and at all heights specified by a Brunt-Väisälä frequency. This initialization also provided the lateral boundary conditions for the entire run – the mountain was deemed far enough from the domain edge for any downstream boundary discontinuities not to have a significant impact on the flow upstream of the barrier on the time scales that the model was run over.

3. Experimental Design

[9] It is hypothesized that the precise shape of Greenland's orography is the cause of the two locations of barrier wind preference. To test this hypothesis, two sets of experiments were run: one with the realistic Greenland orography and the other with modified orography. In the experiments with modified orography, the undulations of the southeast coast were 'filled in' to produce a more uniform coastline (see Figure 2) and allow a direct comparison of the role of the promontories.

[10] The key factors in controlling rotational flow over an isolated mountain are the non-dimensional height, $\hat{h}$, the shape of the obstacle and its orientation relative to the incident wind angle. The non-dimensional mountain height is defined as $\hat{h} = Nh/U$, where N is the Brunt-Väisälä frequency, h is the mountain height and U is the upstream wind speed. This value therefore takes into account not only the mountain's physical height, but also the ability of the ambient flow to undertake vertical motion. Taken together, the shape, non-dimensional height and orientation of the mountain prescribe one, or a combination, of these flow features: mountain waves, wave breaking and flow splitting [*Smith*, 1989; *Ólafsson and Bougeault*, 1996]. In our experiments, the shape of the mountain is fixed as the orography of Greenland, but both the incident wind angle and $\hat{h}$ were varied. Experiments were conducted for incident wind angles between 45° from north (coast parallel) and 180° (beyond coast perpendicular) and a range of $\hat{h}$ between 1.5 and 4.5. The range of $\hat{h}$ was achieved through varying the Brunt-Väisälä frequency and was chosen to encompass the full range of flow regimes explored in previous idealized studies [e.g., *Smith*, 1989; *Ólafsson and Bougeault*, 1996; *Petersen et al.*, 2005].

[11] In all experiments, the model was run for 72 hours. An approximately steady state upstream of the mountain was reached by 48 hours, so an average of the final 24 hours of the model run was analyzed. Many experiments exhibited eddy shedding in the lee of Greenland, but these non-steady state features downstream of the mountain did not have a significant impact on the flow upstream.

4. Results

[12] Results will be presented from two sets of experiments with different $\hat{h}$ which demonstrate the key flow features seen and are representative of a wider range of experiments conducted [see *Harden*, 2012]. Firstly, experiments with a Brunt-Väisälä frequency of 0.01 s^{-1}, a wind

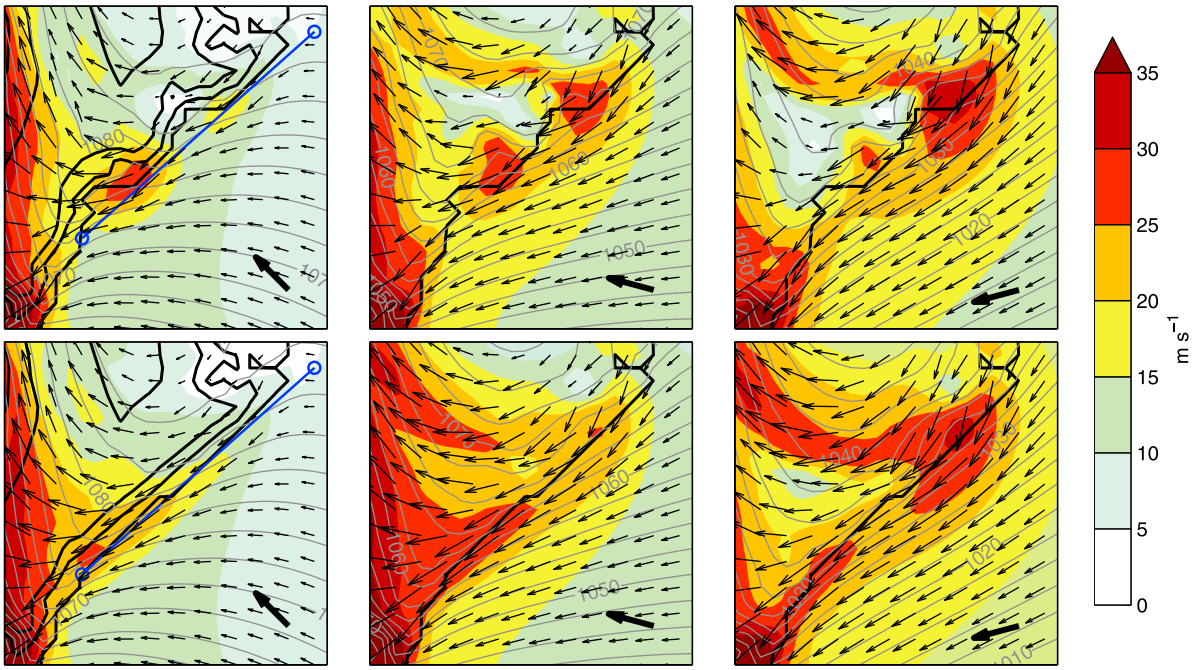

Figure 2. Lowest model level wind speed (colors) and mean sea level pressure (gray contours) for experiments with a Brunt-Väisälä frequency of 0.01 s^{-1} with (top) realistic and (bottom) modified orography. The inflow angles are shown with solid arrows (bottom right) and are (from left to right) 135°, 105° and 75°. The lowest level wind vectors are shown every second grid point. Coastline shown in solid black and orography contours are shown every 1000 m for left hand panels. The blue cross section lines are for Figure 3.

speed of 10 m s^{-1} and incident wind angles of 75°, 105° and 135° are discussed. Note the southeast coast is at approximately 45° from north. Here, using a mountain height of 3000 m, $\hat{h} = 3$. Secondly, experiments with the same incident wind speed and angles but $\hat{h} = 4.5$ (N = 0.015 s^{-1}) will be discussed. Radiosonde observations from the region during barrier wind conditions [see *Harden et al.*, 2011] show low-level Brunt-Väisälä frequencies representative of the experimental range discussed here.

4.1. Small Non-dimensional Mountain Height

4.1.1. General Features

[13] The lowest model level wind fields for experiments with realistic and modified orography are shown in Figure 2. In all experiments, the mountain rotates the upstream flow and creates a coast-parallel jet reminiscent of a barrier wind. Cross mountain sections show that the jets are banked up on the Greenland slope and are generally strongest below mountain height (not shown), providing further evidence that something akin to a barrier flow is being simulated. As with the idealized barrier wind experiments of *Olson and Colle* [2009], the jet width increases as the angle of incidence is reduced, as does the jet magnitude until the angle becomes very shallow.

[14] In all the experiments with realistic orography, two locations of increased wind strength are apparent along the southeast coast. In addition, there exists an omnipresent wind speed maximum at the southwest extreme of the domain which is the signature of a strong easterly tip jet [*Moore and Renfrew*, 2005; *Renfrew et al.*, 2009] formed as the flow reaches the end of the barrier. This feature won't be discussed further in this paper.

[15] The precise positions of the two jet maxima along the southeast coast depends on the angle of wind incidence, but in general they are in agreement with the locations illustrated in Figure 1. The relative strength of the two maxima also changes with incident wind angle – the more northerly location dominates for more northerly (i.e. more acute) flows. In all cases both maxima occur just downstream of the two major promontories along the southeast coast.

[16] In contrast, in the experiments with modified orography the twin maxima largely disappear. This finding is evidence that the precise shape of the orography along the coast of Greenland appears to be the primary factor in determining the location of the strongest winds, in agreement with our initial hypothesis.

[17] These results can also provide some insight into why these regions of enhanced wind occur. The idealized barrier winds simulated in the modified runs (Figure 2, bottom) have similarities with other studies of rotational flow upstream of a mountain [*Ólafsson and Bougeault*, 1997; *Petersen et al.*, 2003, 2005; *Barstad and Grønås*, 2005]. In all cases, a 'left-sided jet' is established along the southeast coast, the velocity of which increases with fetch down the barrier for all but the shallowest angle of incidence. This type of feature can be explained through the adjustment of the upstream geostrophic flow to the presence of the mountain. The decelerating affect of the obstacle reduces the Coriolis force and accelerates the flow to the left (in the Northern Hemisphere) down the pressure gradient as outlined in *Barstad and Grønås* [2005]. The Coriolis force subsequently increases as the flow accelerates. For air that isn't 'blocked' by the mountain, the increased Coriolis force rotates the flow back towards the mountain and the air traverses and scales the barrier. For flow that is

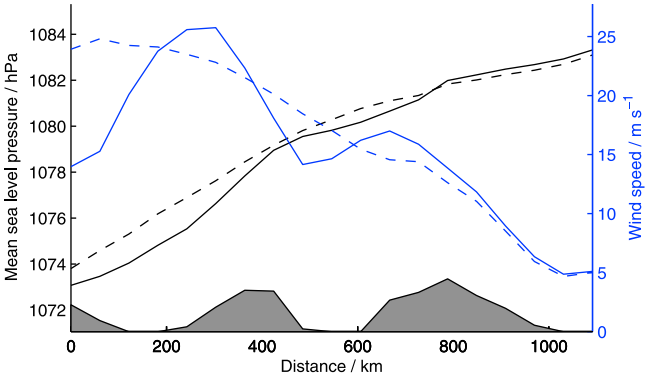

Figure 3. Along-coast mean sea level pressure (black) and lowest model level wind speed (blue) through the jet cores along line shown in left panels of Figure 2 for the experiments with realistic (solid) and modified (dashed) orography for an inflow angle of 135° and $\hat{h}$ = 3. Also shown is the inshore southeast Greenland orography (gray, see Figure 4 for scale). The left of the figure is the southern end of the cross section.

blocked below mountain height a force balance will develop along the coast and the flow will be channeled coast parallel.

[18] There is evidence that much of the flow is escaping up over the barrier in the modified experiments with $\hat{h}$ = 3 especially at the downwind end of the barrier where the mountain height is lower. For example, the flow vectors in Figure 2 are angled up the slope and there are large, low-level vertical velocities in these regions (not shown). The experiments with these flow conditions therefore show flow distortion upstream of the mountain consistent with barrier wind formation with only weak flow blocking. This is consistent with the idealized flow regime of *Petersen et al.* [2005] which states that for $\hat{h}$ = 3 there is marginal flow blocking with some angle dependence.

[19] Bearing this in mind we turn to the realistic orography results and consider what may be inducing the along-coast maxima.

4.1.2. Tip Jet Regime

[20] Easterly tip jets form off the southern tip of Greenland and extend westward out into the Labrador Sea. They form when an upstream coast-parallel flow reaches the end of the barrier. At this location, the along-stream pressure rapidly reduces and the flow accelerates down the pressure gradient. The increase in the Coriolis force and the collapse of the barrier-perpendicular pressure gradient rotates the flow to the right until the flow readjusts to geostrophic balance on the far side of the jet [*Outten et al.*, 2009, 2010]. It is proposed that a similar flow configuration is seen at the two promontories along the southeast Greenland coast.

[21] This easterly tip jet explanation is best exemplified by the experiment pair with a wind angle of 135° (Figure 2, left) through the along-coast mean sea level pressure and the lowest model level wind speed (Figure 3). The modified experiment shows an approximately linear reduction in pressure moving southwestward along the barrier and a corresponding increase in wind speed as the air flows down the pressure gradient. In the experiment with realistic orography the general pattern is similar but superimposed on this are undulations in pressure and wind speed that show up as the regions of enhanced wind in Figure 2. Rapid reductions in pressure occur just downwind of the promontories in the orography in conjunction with the two regions of increased wind speed. This is very similar to what occurs for the flow into an easterly tip jet at Cape Farewell [*Outten et al.*, 2009, 2010]. The pressure is reduced downstream of the promontory due to the inward undulation of the barrier and the flow consequently accelerates down this steeper pressure gradient and a tip jet is formed. The flow in this jet will rotate to the right as the Coriolis force dominates the cross stream force balance. Evidence of this rotation can be seen in the flow field of Figure 2. This tip-jet-like flow can also be seen in the other experiments with reduced inflow angles although another feature becomes increasingly apparent – downslope winds triggered by mountain waves.

4.1.3. Mountain Waves

[22] Mountain waves can be triggered when stable flow is forced over relatively steep orography [*Smith*, 1989; *Doyle et al.*, 2005]. They manifest themselves as static, upward propagating gravity waves in the free atmosphere and the resulting low-level flow on the lee side of the mountain is strongly downslope [*Durran*, 1990].

[23] From a coast-parallel viewpoint, the aforementioned promontories along the southeast coast form a series of mountains (see Figure 4). There appears to be mountain waves over both promontories in the realistic experiment shown, as seen by the coherent vertical undulations in the isentropes and associated wind speed maxima on the lee side. These features are not apparent in the experiment with modified orography. Mountain waves and downslope acceleration are seen in all the realistic orography experiments, the only difference being the relative strength of waves over each peak, which is inflow-angle dependent. The

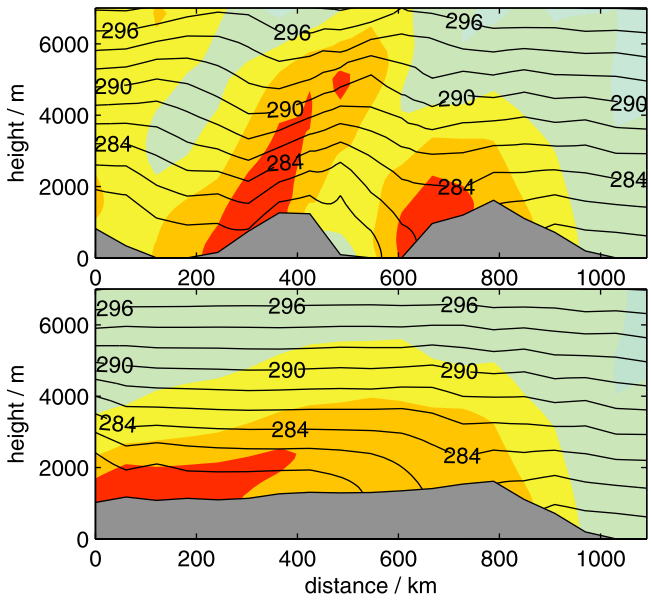

Figure 4. Cross section of horizontal wind speed (colors, scale as Figure 2) and potential temperature (contours) taken through a line 70 km inshore of the blue cross section line shown in Figure 2 for the experiments with (top) realistic and (bottom) modified orography, an inflow angle of 105° and $\hat{h}$ = 3.

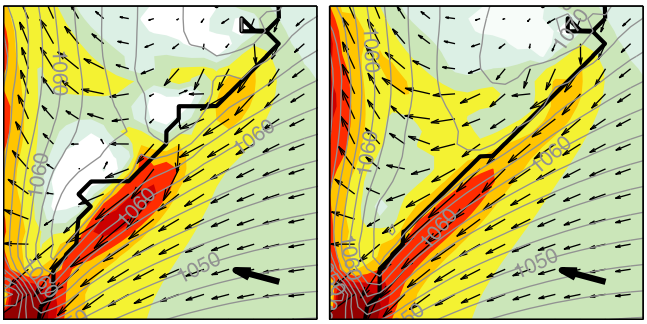

Figure 5. As Figure 2 but for the experiments with (left) realistic and (right) modified orography, an inflow angle of 105° and $\hat{h} = 4.5$.

lee side accelerations contribute to the low-level bullets of enhanced wind seen in the near surface fields (Figure 2). To the authors knowledge this is the first description of north-easterly mountain waves along the southeast coast of Greenland.

[24] Even for the experiments with modified orography there is evidence for some mountain waves and lee side acceleration; flow with a strong northerly component sees the eastern corner of Greenland (where Scoresbysund would be found) as an isolated mountain and triggers mountain waves and a strong downslope flow. This accounts in part for the wind speed maxima found here in experiments with shallower inflow angles (Figure 2), although the tip jet mechanism is also likely to be important at this 'corner' of Greenland.

4.2. Large Non-dimensional Mountain Height

[25] For experiments with a Brunt-Väisälä frequency of 0.015 s^{-1} the non-dimensional mountain height is 4.5. This is large enough, in theory, to induce strong flow blocking regardless of incident wind direction [*Petersen et al.*, 2005]. Figure 5 shows that the low-level flow from both realistic and modified experiments with a wind angle of 105° is indeed significantly blocked by the mountain. The jet maxima are no longer banked against the slope and low-level vertical velocities (not shown) are negligible on the slope.

[26] In experiments with enhanced blocking, gravity waves and the associated lee-side winds are inhibited. There are still regions of enhanced wind speed (e.g., Figure 5), but these are likely the effect of the tip jet mechanism alone. In general, the realistic and modified experiments differ by a smaller amount. It appears that the effect of greater blocking is to reduce how much the flow is influenced by variations in the coastline.

5. Conclusions

[27] The aim of this study was to understand why there are two locations of enhanced high wind activity along the southeast coast of Greenland. Through idealized modeling, the two regions of enhanced winds have been reproduced and found to only occur when the undulations in the southeast coast are resolved. This confirms our hypothesis that it is the promontories along Greenland's coast which are the primary cause for the spatial distribution of barrier winds.

[28] Two mechanisms for the existence of these maxima have been proposed. Firstly, low-level flow passing along the southeast coast can be accelerated due to the reduction in pressure downstream of the two major promontories, similar to the dynamics involved in the production of easterly tip jets at Cape Farewell [*Outten et al.*, 2009, 2010]. Secondly, any barrier parallel component of the flow is capable of triggering mountain waves and strong low-level downslope winds in the lee of the promontories. Both mechanisms were seen most strongly in experiments with moderate static stability that only allowed for weak upstream blocking of the flow. For experiments with higher upstream static stability a larger degree of blocking was observed and the flow felt the effect of the coastal undulations more weakly.

[29] There are clearly limitations to the modeling study presented that restrict like-for-like comparisons with 'real world' barrier winds. For example, the effect of surface friction and heat fluxes has been negated. The 3-D structure of mid-latitude cyclones is likely to also be important in the specific location and mechanisms for barrier wind formation. Extending this study to address these limitations is reserved for future work.

[30] **Acknowledgments.** The authors would like to acknowledge discussions of the central hypothesis examined in this study with G. W. K. Moore and G. N. Petersen and would like to thank NCAS for the access to, and assistance with running, the Unified Model.

[31] The Editor thanks the anonymous reviewer for assistance in evaluating this paper.

References

Barstad, I., and S. Grønås (2005), Southwesterly flows over southern Norway—Mesoscale sensitivity to large-scale wind direction and speed, *Tellus, Ser. A*, *57*, 136–152, doi:10.1111/j.1600-0870.2005.00112.x.

Doyle, J. D., M. A. Shapiro, Q. Jiang, and D. L. Bartels (2005), Large-amplitude mountain wave breaking over Greenland, *J. Atmos. Sci.*, *62*, 3106–3126, doi:10.1175/JAS3528.1.

Durran, D. R. (1990), Mountain waves and downslope winds, *Atmos. Processes Complex Terrain*, *23*, 59–83.

Haine, T. W. N., S. Zhang, G. W. K. Moore, and I. A. Renfrew (2009), On the impact of high-resolution, high-frequency meteorological forcing on Denmark Strait ocean circulation, *Q. J. R. Meteorol. Soc.*, *135*, 2067–2085, doi:10.1002/qj.505.

Harden, B. E. (2012), Barrier winds off southeast Greenland and their impact on the ocean, PhD thesis, Univ. of East Anglia, Norwich, U. K.

Harden, B. E., I. A. Renfrew, and G. N. Petersen (2011), A climatology of wintertime barrier winds off southeast Greenland, *J. Clim.*, *24*, 4701–4717, doi:10.1175/2011JCLI4113.1.

Hastings, D. A., et al. (1999), The Global Land One-kilometer Base Elevation (GLOBE) digital elevation model, version 1.0., technical report, Natl. Geophys. Data Cent., NOAA, Boulder, Colo.

Moore, G. W. K., and I. A. Renfrew (2005), Tip jets and barrier winds: A QuikSCAT climatology of high wind speed events around Greenland, *J. Clim.*, *18*, 3713–3725, doi:10.1175/JCLI3455.1.

Moore, G. W. K., R. S. Pickart, and I. A. Renfrew (2008), Buoy observations from the windiest location in the world ocean, Cape Farewell, Greenland, *Geophys. Res. Lett.*, *35*, L18802, doi:10.1029/2008GL034845.

Ólafsson, H., and P. Bougeault (1996), Nonlinear flow past an elliptic mountain ridge, *J. Atmos. Sci.*, *53*, 2465–2489.

Ólafsson, H., and P. Bougeault (1997), The effect of rotation and surface friction on orographic drag, *J. Atmos. Sci.*, *54*, 193–210.

Olson, J. B., and B. A. Colle (2009), Three-dimensional idealized simulations of barrier jets along the southeast coast of Alaska, *Mon. Weather Rev.*, *137*, 391–413, doi:10.1175/2008MWR2480.1.

Outten, S. D., I. A. Renfrew, and G. N. Petersen (2009), An easterly tip jet off Cape Farewell, Greenland. II: Simulations and dynamics, *Q. J. R. Meteorol. Soc.*, *135*, 1934–1949, doi:10.1002/qj.531.

Outten, S. D., I. A. Renfrew, and G. N. Petersen (2010), Erratum: An easterly tip jet off Cape Farewell, Greenland. II: Simulations and dynamics, *Q. J. R. Meteorol. Soc.*, *136*, 1099–1101, doi:10.1002/qj.629.

Petersen, G. N., and I. A. Renfrew (2009), Aircraft-based observations of air-sea fluxes over Denmark Strait and the Irminger Sea during high wind speed conditions, *Q. J. R. Meteorol. Soc.*, *135*, 2030–2045, doi:10.1002/qj.355.

Petersen, G. N., H. Ólafsson, and J. E. Kristjánsson (2003), Flow in the lee of idealised mountains and Greenland, *J. Atmos. Sci.*, *60*, 2183–2195.

Petersen, G. N., J. E. Kristjánsson, and H. Ólafsson (2005), The effect of upstream wind direction on atmospheric flow in the vicinity of a large mountain, *Q. J. R. Meteorol. Soc.*, *131*, 1113–1128, doi:10.1256/qj.04.01.

Petersen, G. N., I. A. Renfrew, and G. W. K. Moore (2009), An overview of barrier winds off southeastern Greenland during GFDEx, *Q. J. R. Meteorol. Soc.*, *135*, 1950–1967, doi:10.1002/qj.455.

Renfrew, I. A., et al. (2008), The Greenland Flow Distortion Experiment, *Bull. Am. Meteorol. Soc.*, *89*, 1307–1324, doi:10.1175/2008BAMS2508.1.

Renfrew, I. A., S. D. Outten, and G. W. K. Moore (2009), An easterly tip jet off Cape Farewell, Greenland. I: Aircraft observations, *Q. J. R. Meteorol. Soc.*, *135*, 1919–1933, doi:10.1002/qj.513.

Smith, R. B. (1989), Hydrostatic airflow over mountains, *Adv. Geophys.*, *31*, 1–41, doi:10.1016/S0065-2687(08)60052-7.

Straneo, F., G. S., et al. (2010), Rapid circulation of warm subtropical waters in a major glacial fjord in East Greenland, *Nature Geosci.*, *3*, 182–186, doi:10.1038/ngeo764.

Våge, K., T. S. Spengler, H. C. Davies, and R. S. Pickart (2009), Multi-event analysis of the westerly Greenland tip jet based upon 45 winters in ERA-40, *Q. J. R. Meteorol. Soc.*, *135*, 1999–2011, doi:10.1002/qj.488.